# Synthesis of Monolayer SiP by Chemical Vapor Transport toward Superior Optoelectronic and Catalytic Performance

## Supporting information

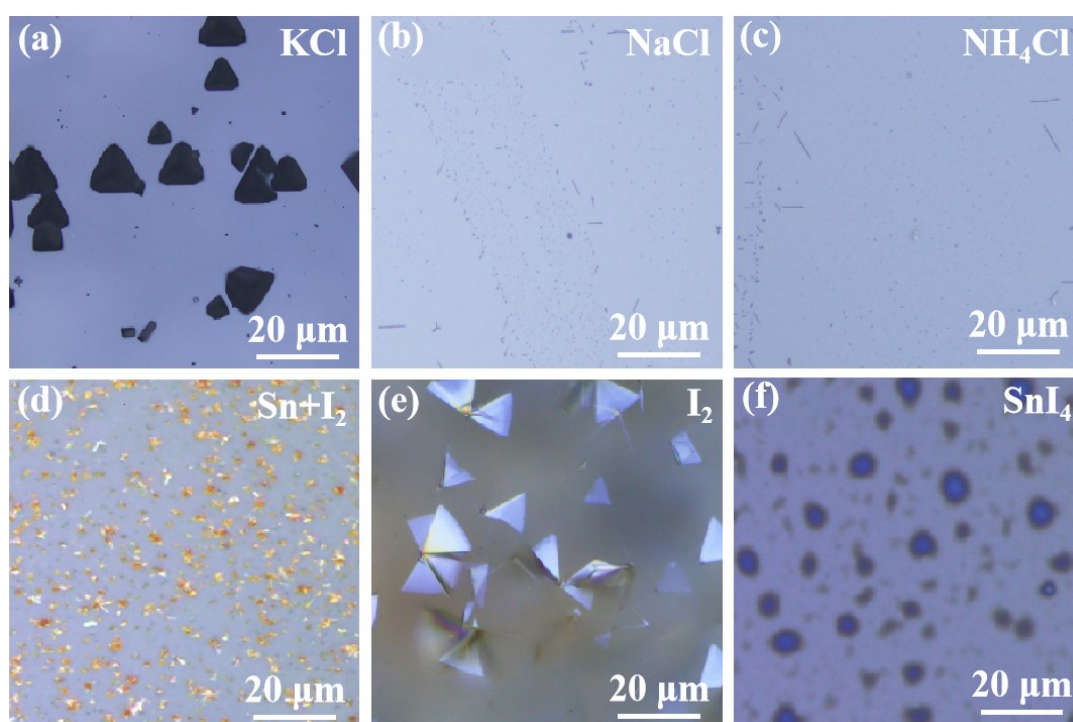Tong Yu [a], Hailong Qiu*[a], Hongjun Liu [a], Zhanggui Hu [a] and Yicheng Wu [a]

**Fig. S1** Optical image of 2D SiP nanosheets prepared using different transport agents on mica substrates. (a) KCl, (b) NaCl, (c) $NH_4Cl$, (d) $Sn+I_2$, (e) $I_2$, (f) $SnI_4$.

We used KCl、 NaCl、 $NH_4Cl$、 $Sn+I_2$、 $I_2$, and $SnI_4$ as transport agents to study the preparation of 2D SiP nanosheets. Fig. S1(a) shows that when KCl was used as a transport agent, black conical substances were found on the mica substrate, which may be caused by the reaction between KCl and P to generate water-soluble $KPCl_2$.[1] When NaCl and $NH_4Cl$ were selected as transport agents, as shown in Fig. S1(b) and (c), no SiP generation was found on mica substrate, which may be due to the unsatisfactory transport effect of halogen Cl on SiP. In the Si, P, and $I_2$ reaction

system, we tried adding flux Sn to improve the experiment. As shown in Fig. S1(d), we found many SiP particles deposited on the mica substrate because the environment inside the quartz tube was changed after adding Sn, and the reactants were more easily transported to the growth zone by the transport agent. Because the transport rate did not match the growth rate of the SiP crystal material, SiP grew in an "island style." Finally, it is deposited on the mica substrate in granular form. $I_2$ is one of the most common transport agents in CVT synthetic crystal materials due to its ability to sublimate at room temperature. Fig. S1(e) shows that when $I_2$ is used as a transport agent, high-quality 2D SiP nanosheets can be obtained on mica substrates. Given the results of the Si, P, $I_2$, and Sn reaction systems, we used $SnI_4$ as the transport agent. As shown in Fig. S1(f), we found traces of etching on the surface of the mica substrate, which showed that $SnI_4$ had a strong etching effect on mica. In conclusion, $I_2$ is the most suitable transport agent for preparing 2D SiP crystals using the CVT method.
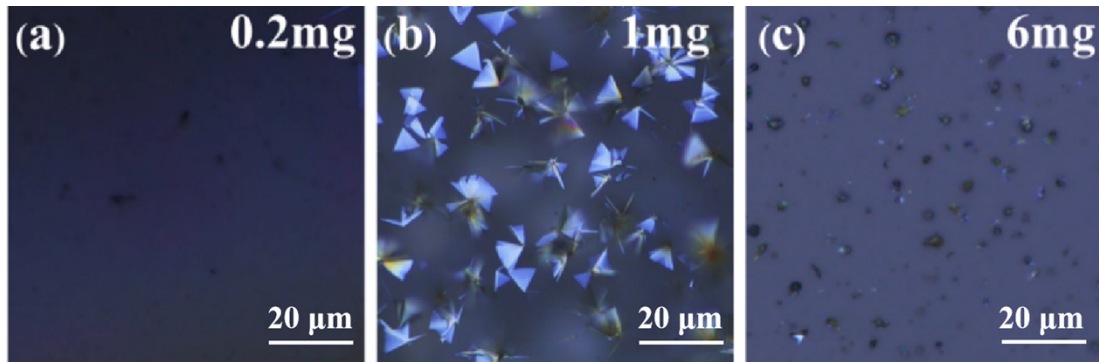


**Fig. S2.** Optical images of 2D SiP nanosheets were prepared with different $I_2$ contents on mica substrates. (a) 0.2 mg, (b) 1 mg, (c) 6mg.

Appropriate transport dose is also an essential factor affecting the preparation of 2D SiP nanosheets by the CVT method. Because the amount of transport agent is closely related to the total pressure of the system when the transport dose is too large, the total pressure of the reaction system increases, resulting in poor transport effect of the transport agent, and the target sample cannot be obtained; If the transport dose is too small, a reversible air pressure balance cannot be formed in the system, which

leads to the transport agent cannot play the transport effect, and the target sample cannot be obtained. The reversible air pressure cycle can be achieved in the quartz tube only by selecting the appropriate transport dose. That is, there will be a reversible balance inside, which makes the transport of the transport agent match the growth of the growth zone, and then the target sample can be obtained. To confirm this, we used different amounts of transport agents to prepare 2D SiP nanosheets. It can be observed in Fig. S2(a) that when 0.2 mg of $I_2$ is added to the reaction system, due to the small transport dose, a practical transport effect cannot be formed inside the quartz tube, failing to prepare 2D SiP nanosheets on the mica substrate successfully; It can be observed in Fig. S2(b) that when 1 mg $I_2$ is added, 2D SiP nanosheets can be successfully prepared on mica substrate due to the formation of an effective reversible equilibrium inside the container. It can be observed in Fig. S2(c) that when the amount of $I_2$ increases to 6 mg, due to the high internal pressure of the quartz tube, effective transport cannot be formed, so 2D SiP nanosheets cannot be observed on the mica substrate. In conclusion, 2D SiP nanosheets are most easily prepared when transport agent $I_2$ is 1mg.
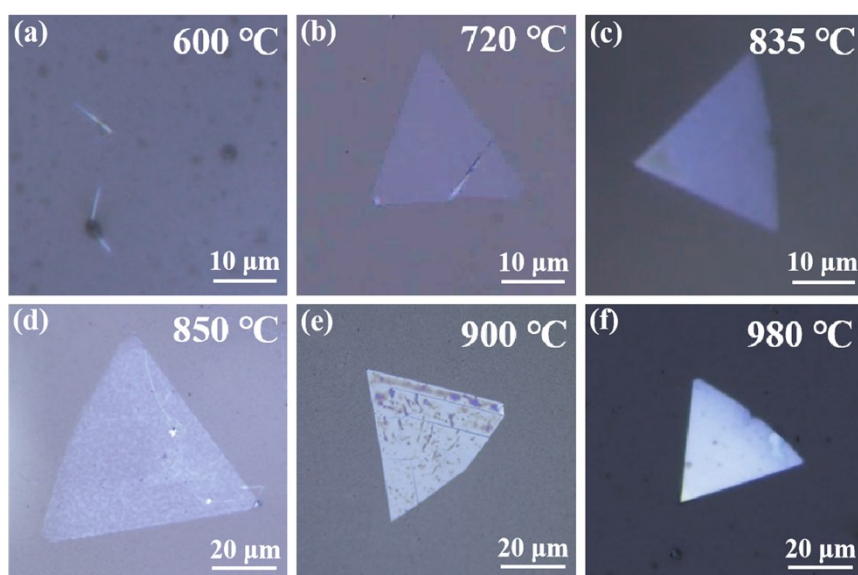


**Fig. S3.** Optical images of 2D SiP nanosheets were prepared at different growth temperatures on mica substrates. (a) 600℃, (b) 720℃, (c) 835℃, (d) 850℃, (e)

900℃, (f) 980℃.

In the preparation of 2D SiP nanosheets by the CVT method, the temperature of the reaction zone determines whether the transport agent can react with the reactants, while the growth temperature affects the nucleation and growth of 2D SiP nanosheets on mica substrates. Therefore, we investigated the preparation of 2D SiP nanosheets at 600℃~980℃ in the growing region, as shown in Fig S3. When the temperature in the growing region is low, the temperature gradient in the quartz tube is large, resulting in the reactants Si powder and P powder not reacting with the transport agent $I_2$ to generate 2D SiP nanosheets. As the temperature in the growing region increases, the temperature gradient in the quartz tube decreases, and the size of 2D SiP nanosheets increases. However, when the temperature in the growing region is too high, the diffusion rate is too fast, which makes the diffusion rate of SiP larger than the growth rate and eventually leads to thicker SiP nanosheets. Therefore, when the temperature of the growing region is 850℃, 2D SiP nanosheets with large sizes can be obtained.
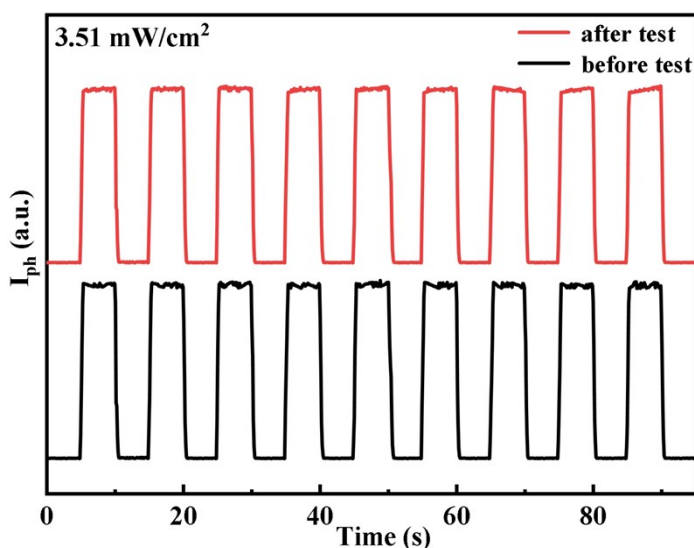


**Fig. S4** Time-resolved light response curves before and after changing the power density when the optical power density is 3.51 mW/cm$^2$.

Table S1 Rise and decay time of photodetectors of different two-dimensional materials.

| Materials | Preparation method | Excitation Wavelength | Response time | Ref |
|---|---|---|---|---|
| WS$_2$ | PLD | 635 nm | $\tau_{rise}$=4.1 s $\tau_{decay}$=4.4 s | [2] |
| ReS$_2$ | CVD | 500 nm | $\tau_{rise}$=0.82 s $\tau_{decay}$=0.62 s | [3] |
| SnS$_2$ | Ethanol thermal | 405 nm | $\tau_{rise}$=0.82 s $\tau_{decay}$=0.62 s | [4] |
| HfS$_2$ | CVD | 420 nm | $\tau_{rise}$=55 ms $\tau_{decay}$=78 ms | [5] |
| SiP | Flux method | 365 nm | $\tau_{rise}$=60 s $\tau_{decay}$=30 s | [6] |
| SiP | Mechanical exfoliation | 671 nm | $\tau_{rise}$=500 ms $\tau_{decay}$=540 ms | [7] |
| SiP | CVT | 450 nm | $\tau_{rise}$=11.5 ms $\tau_{decay}$=18.5 ms | This work |
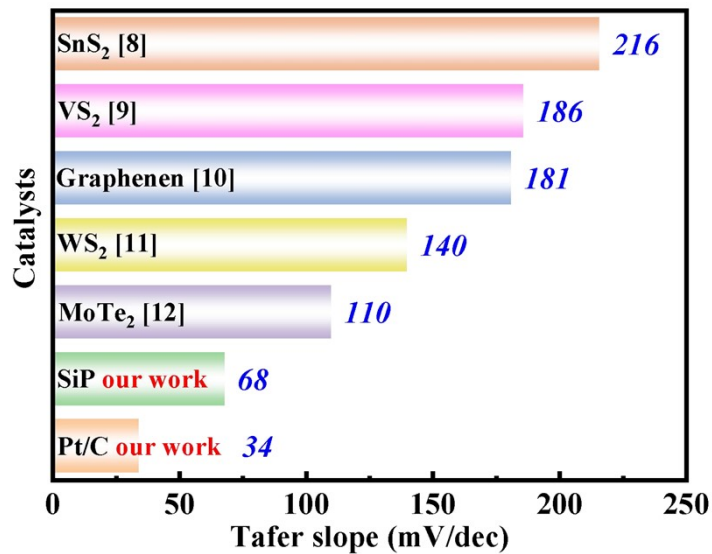
**Fig. S5.** The HER properties of SiP and other 2D materials were compared at 0.5 mol/L $H_2SO_4$.
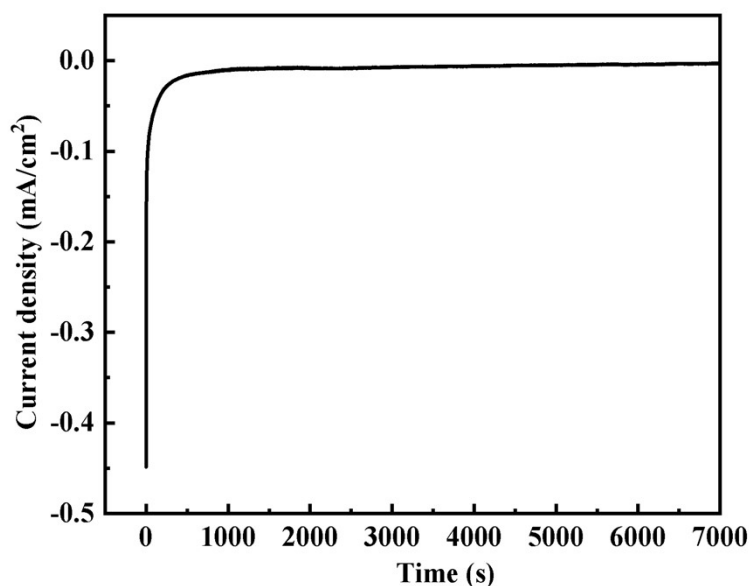


**Fig. S6.** The i-t measurements.

## References

1.  A. J. Mannix, B. Kiraly, B. L. Fisher, M. C. Hersam, N. P. Guisinger, Silicon Growth at the Two-Dimensional Limit on Ag(111), *Acs Nano*, 2014, **8**, 7538-7547.

2.  J. D. Yao, Z. Q. Zheng, J. M. Shao, G. W. Yang, Stable, highly-responsive and broadband photodetection based on large-area multilayered $WS_2$ films grown by pulsed-laser deposition, *Nanoscale*, 2015, **7**, 14974-14981.

3.  M. Hafeez, L. Gan, H. Li, Y. Ma, T. Zhai, Large-Area Bilayer $ReS_2$ Film/Multilayer $ReS_2$ Flakes Synthesized by Chemical Vapor Deposition for High Performance Photodetectors, *Adv. Funct. Mater.* 2016, **26**, 4551-4560.

4.  Y. Tao, X. Wu, W. Wang, J. Wang, Flexible photodetector from ultraviolet to near infrared based on a $SnS_2$ nanosheet microsphere film, *J. Mater. Chem. C*, 2015, **3**, 1347-1353.

5.  C. Yan, L. Gan, X. Zhou, J. Guo, W. Huang, J. Huang, B. Jin, J. Xiong, T. Zhai, Y. Li, Space-Confined Chemical Vapor Deposition Synthesis of Ultrathin $HfS_2$ Flakes for Optoelectronic Application, *Adv. Funct. Mater.,* 2017, **27,** 1702918.

6.  S. Zhao, P. Luo, S. Yang, X. Zhou, Z. Wang, C. Li, S. Wang, T. Zhai, X. Tao, Low-Symmetry and Nontoxic 2D SiP with Strong Polarization-Sensitivity and Fast Photodetection. *Adv. Opt. Mater.*, 2021, **9**, 2100198.

7.  C. Li, S. Wang, X. Zhang, N. Jia, T. Yu, M. Zhu, D. Liu, X. Tao, Controllable seeded flux growth and optoelectronic properties of bulk o-SiP crystals, *CrystEngComm*, 2017, **19**, 6986-6991.

8.  G. Shao, H. Xiang, M. Huang, Y. Zong, J. Luo, Y. Feng, X.-X. Xue, J. Xu, S. Liu and Z. Zhou, S vacancies in 2D $SnS_2$ accelerating hydrogen evolution reaction, *Sci. China. Mater.*, 2022, **65**, 1833-1841.

9.  K. Karthick, T. K. Bijoy, A. Sivakumaran, A. B. M. Basha, P. Murugan and S. Kundu, Enhancing Hydrogen Evolution Reaction Activities of 2H-Phase $VS_2$ Layers with Palladium Nanoparticles, *Inorg. Chem.*, 2020, **59**, 10197-10207.

10. J. Muthu, F. Khurshid, H.-T. Chin, Y.-C. Yao, Y.-P. Hsieh and M. Hofmann, The HER performance of 2D materials is underestimated without morphology correction, *Chem. Eng. J.*, 2023, **465**, 142852.

11. H. Wang, Z. Xu, Z. Zhang, S. Hu, M. Ma, Z. Zhang, W. Zhou and H. Liu, Addressable surface engineering for N-doped $WS_2$ nanosheet arrays with abundant active sites and the optimal local electronic structure for enhanced hydrogen evolution reaction, *Nanoscale*, 2020, **12**, 22541-22550.

12. P. V. Shinde, P. Mane, D. J. Late, B. Chakraborty and C. S. Rout, Promising 2D/2D $MoTe_2/Ti_3C_2T_x$ Hybrid Materials for Boosted Hydrogen Evolution Reaction, *ACS Appl. Energy Mater.*, 2021, **4**, 11886-11897.